

Photonic jet: direct micro–peak machining

Robin Pierron^{†*}, Pierre Pfeiffer[†], Grégoire Chabrol^{†‡}, Sylvain Lecler[†]

Article published in *Applied Physics A* 123, 686 (2017)

<https://doi.org/10.1007/s00339-017-1319-1>

Abstract

We report on the first evidence of direct micro–peak machining using a photonic jet (PJ) with nanosecond laser pulses. PJ is a high concentrated propagative light beam with a full width at half maximum (FWHM) smaller than the diffraction limit. In our case, PJs are generated with a shaped optical fiber tip. Micro–peaks with a FWHM of around 1 μm , a height until 590 nm and an apex radius of 14 nm, were repeatability achieved on a silicon wafer. The experiments have been carried out in ambient air using a 100/140 multimode silica fiber with a shaped tip along with a 35 kHz pulsed laser emitting 100 ns pulses at 1064 nm. This study shows that the phenomenon occurs only at low energies, just under the ablation threshold. Bulk material appears to have moved around to achieve the peaks in a self–organized process. We hypothesize that the matter was melted and not vaporized; hydrodynamic flow of molten material governed by surface–tension forces may be the causes. This surface modification has many applications. For example, this paper reports on the decrease of wettability of a textured silicon wafer.

Keywords: self–organized micro–spikes, photonic jet, shaped optical fiber tip, multimode fiber, wettability

1 Introduction

Direct laser subwavelength micromachining is currently a challenging topic. Photonic jets have already demonstrated the ability to reduce the laser etching size beyond the diffraction limit using micro–beads [1, 2, 3, 4, 5, 6] or more recently using shaped optical fiber tips [7, 8, 9]. A Photonic jet (PJ) is a high concentrated propagative light beam with a full width at half maximum (FWHM) smaller than the diffraction limit [10, 11, 12, 13]. The power density can be more than 200 times higher than the one of the incident wave [1, 11, 14]. To achieve PJ, shaped fiber tips are obviously easier to move than a microsphere and therefore, to implement in an industrial process. Moreover, the fiber tips have no contact with the processed surface and are not altered by the removed material [7, 8, 9]. Until now, only sub–micro PJ etching was reported. Micro–peaks formation was reported for processes using femtosecond laser pulses on thin metal and silicon films [15, 16, 17, 18, 19, 20]. Micro–peaks were also generated using nanosecond laser pulses on thin gold film [21, 22], but never on silicon bulk.

In this paper, we report for the first time the possibility to achieve direct micro–peaks surface texturing using nanosecond pulses. Taking advantage of the photonic jet at the exist of a shaped optical fiber tip, peaks with a FWHM of around 1 μm , a height of almost

[†]ICube Laboratory, University of Strasbourg, CNRS UMR 7357, 300 Bd. Sébastien Brant, 67412 Illkirch, France

[‡]ECAM Strasbourg–Europe, 2 Rue de Madrid, 67012 Schiltigheim, France

*Corresponding author: robin.pierron@unistra.fr

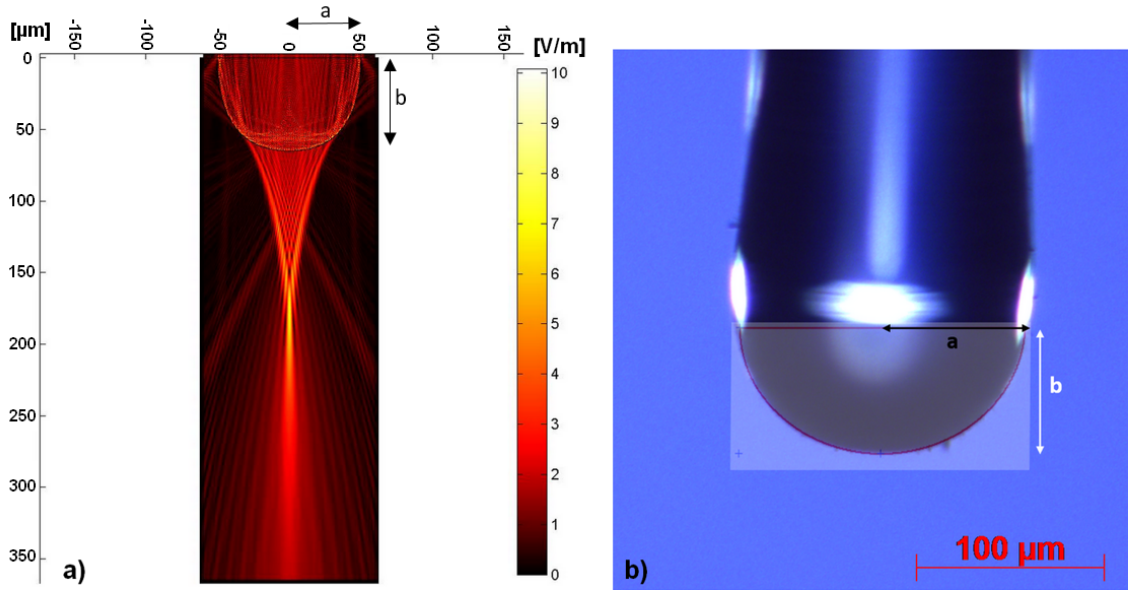


Figure 1: a) Simulation of the electrical field norm through and outside of the shaped silica fiber tip ($a = 50 \mu\text{m}$, $b = 63 \mu\text{m}$, $w_0 = 1$) excited by the fundamental mode of the fiber. b) Optical microscope view of the shaped fiber tip ($a = 80 \mu\text{m}$, $b = 63 \mu\text{m}$, $w_0 = 1$).

an half micrometer and an apex radius of fews ten nanometers, were repeatably achieved on a silicon wafer. Surfaces with micro-peaks can have a wide range of applications. For example, A few millimeter squares surface with micro–spikes has shown an decrease of wettability.

2 Experiment details

The laser source is a commercial near–infrared pulsed laser (VGEN ISP 1-40-30) emitting at 1064 nm with pulses of 100 ns at a repetition rate of 35 kHz. The output beam has a diameter of 6 mm at $1/e^2$ and a beam quality factor (M^2) of 1.3. This corresponds to a quasi–Gaussian beam profile. An achromatic doublet, with a focal length of 19 mm, couples the laser beam into the fiber, whose position is controlled by XYZ microstages.

The fiber system is a multimode step–index silica fiber with a core diameter of $100 \mu\text{m}$ and a cladding diameter of $140 \mu\text{m}$. The numerical aperture (NA) is 0.22. The tip shape is numerically described by a Bézier curve set by a base radius ($a = 50 \mu\text{m}$), a tip length ($b = 63 \mu\text{m}$) and a Bézier weight ($w_0 = 1$) [7]. It has been designed to achieve photonic jet of around $1 \mu\text{m}$ at a distance of around $100 \mu\text{m}$ of the tip when excited by the fundamenal mode (Fig. 1 a). The numerical method is described in [7, 8, 9]. The tip has been achieved by LovaLite using an electric–arc thermoforming technique [23]. The result has a base radius a slightly larger due the cladding: $a \simeq 80 \mu\text{m}$ (Fig. 1 b).

The shaped optical fiber tip is placed orthogonal to the sample. The fiber position is controlled by a Z–motorized stage and the sample position by XY–motorized stages. The distance between the tip and the sample is controlled by a camera with a 5x telecentric objective thanks to an image processing based on the reflectance of the tip into the sample. The laser, the motorized stages and the camera processing are controlled by LabView. The experiences are carried out at ambient atmosphere conditions. The power at the outputs of the laser and the fiber tip has been measured with a calorimeter Ophir Vega with a 12A–P sensor.

In the following we name working distance the distance between the tip end and the maximum of intensity of the photonic jet. Experimentally, when both the laser pulse energy and the distance between the tip and the sample vary, the working distance corresponds to the distance for which the smallest mark is achieved with the smallest energy. It is intrinsic to the fiber tip and has been determined experimentally in our previous work to be $100 \pm 2 \mu\text{m}$ for the tip shown in Fig. 1 b) [9] not far from the $113 \mu\text{m}$ predicted by simulation (Fig.1 a). Our experiments have shown that this working distance is enough to avoid the re-deposition of melt material on the fiber tip if material is ablated. This also allows ensure the tip integrity during the motion control: no shock and easier control due the $2 \mu\text{m}$ PJ positioning tolerance. From simulations, we can give some general rules: (1) Photonic jet with the same FWHM (Full Width at Half Maximum) can be obtained at larger working distance using larger optical fiber core. However, in this case more energy is required to achieve the same process. Namely, it is not so easy to couple energy in the fundamental mode. (2) For a given fiber radius, generally the working distance is larger increasing the Bézier weight (w_0) or decreasing the tip length (b). However, the photonic jet FWHM increases. Therefore this tip was a good compromise.

The sample is a monocrystalline silicon wafer with a passive layer (thickness of approximately 2 nm) and an initial roughness of $2 \pm 1 \text{ nm}$. For each laser irradiation, 35 pulses have been used. Before and after the laser process, the sample was cleaned and dried with alcohol and dry air.

The micro-peaks have been characterized with two different methods: a white light interferometric microscope and an atomic force microscope (AFM). The interferometric system based on coherence scanning interferometry was a Zygo NewView 7200 profilometer with an axial resolution of 3 nm and a lateral resolution of 550 nm (50x Mirau objective, $\text{NA} = 0.55$). The AFM, a Park Systems XE-70 isolated inside an acoustic enclosure, worked in the non-contact mode. The field size used was $20 \times 20 \mu\text{m}$ with a lateral resolution of 39 nm and a axial resolution of 2 nm .

The wettability of the flat and fakir's bed of nails-like textured sample was measured with a Krüss Drop Shape Analyser DSA25. Static contact angle were measured with around $10 \mu\text{L}$ distilled water droplets by the sessile drop method. A computation method based on the analysis of the droplet shape determined by the model of Laplace-Young was used.

3 Results and discussion

A $110 \times 100 \mu\text{m}$ matrix with peaks every $5 \mu\text{m}$ has been achieved on silicon. In Fig. 2, the 3D view obtained by the interferometric microscope shows that micro-peak machining by PJ with an shaped optical fiber tip is a repeatable process. The measured mean height for 30 peaks was $354 \pm 3 \text{ nm}$, the mean FWHM was $1 \pm 0.6 \mu\text{m}$ and the maximum height was $590 \pm 3 \text{ nm}$. Thus, peaks have a width larger than their height. Pay attention, due to the scales, the aspect ratio of the micro-peaks are different from what appears in Fig. 3.

The PJ micro-peaks were obtained with 35 pulses, that corresponded to our minimum controlable number of pulses. The laser source has a minimum repetition rate of 35 kHz and its minimum controllable shot time is 1 ms . The energy per pulse was $30 \mu\text{J}$. Peak formation occurs only when the pulse energy is just under the ablation threshold ($36 \mu\text{J}$ with our experimental conditions [9]). For comparison purposes, the dimensions of a PJ ablation has been measured. An example of ablation with 35 pulses with a pulse energy of $36 \mu\text{J}$ has been achieved (cf. Fig. 3 b)). The PJ ablation is a sub-micro ablation with a deep of $456 \pm 3 \text{ nm}$ and a FWHM of $0.9 \pm 0.6 \mu\text{m}$. An example of a PJ peak from the matrix is presented (cf. Fig. 3 a)). The PJ peak is a sub-micro peak with a height of $403 \pm 3 \text{ nm}$

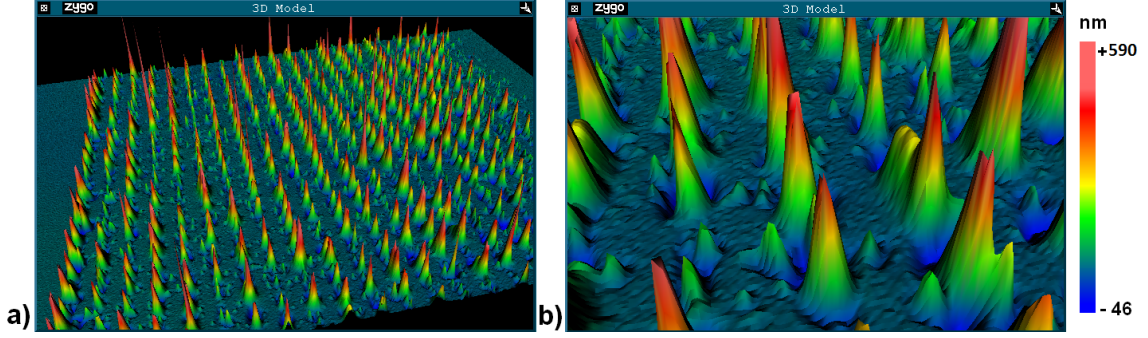


Figure 2: 3D view with Zygo profilometer. a) $110 \times 110 \mu\text{m}$ matrix on silicon with peaks every $5 \mu\text{m}$; 35 pulses for each PJ peaks; pulse energy of $30 \mu\text{J}$ — b) Zoom. Note that the unit lengths are not the same in the transverse plane and for height.

and a FWHM of $1.3 \pm 0.6 \mu\text{m}$. Hence, the PJ peak has a FWHM with the same order magnitude (around $1 \mu\text{m}$) as the FWHM of the PJ ablation, which is also the width of the PJ.

If a different distance between the tip and the sample is used, as illustrated in Fig. 3 c) with $110 \mu\text{m}$, no more peaks are generated. The affect area (around $17 \mu\text{m}$) has several maxima and minima and the highest maximum (around 120 nm) is not so high as the peaks and has a FWHM of $4 \mu\text{m}$. This confirms the role of PJ in the peak generation.

In order to confirm the interferometer results, a micro-peak has been measured by AFM (cf. Fig. 4). A height of $335 \pm 2 \text{ nm}$ and a FWHM of $1.330 \pm 0.040 \mu\text{m}$ have been measured (cf. Fig. 5). The micro-peak has a quasi-conical shape with an apex radius of $14 \pm 2 \text{ nm}$. Thus, with a small deviation (inferior to 10%), the AFM measurement confirms the interferometer profiles.

The physical mechanisms of the micro-peak formation are hypothetical. A similar phenomenon is the micro-peak formation on thin metal films by femtosecond lasers [16, 17, 18, 20]. The absorption processes are very different, however the properties of the PJ (characteristic sizes) allow interaction with a volume of matter similar to the case of femtosecond laser. In the two cases, the micro-peaks are generated by fluences just below the ablation threshold. Independently of the peaks, under nanosecond laser irradiation, melt dynamics is a dominant mechanism; femtosecond irradiation induces more complex dynamics including thermoplastic deformation [17]. In silicon, as with femtosecond pulses, the formation mechanism of the micro-peaks could be apparently due to the hydrodynamic flow of molten material governed by surface-tension forces. The mechanism is due to the thermal expansion of the heated solid part of the material. This thermal extension induces stresses, which provide forces directly perpendicular to the solid-liquid interface. Theses forces push the melted material towards the center of the irradiated region. The peak formation would be arrested by the surface tensions forces and material solidification [17, 20].

An interest in microstructured surfaces with peaks has arisen thanks to the superhydrophobic effect [24, 25]. As an application example, a $5 \times 5 \text{ mm}$ matrix with micro-peaks every $50 \mu\text{m}$, called fakir's bed of nails surface, has been achieved on silicon. A wettability test has been carried on the non-textured surface and textured surface (cf. Fig. 6) with a drop of water. When the contact angle is below 90 degrees, the surface is considered hydrophilic. On the opposite, above 90 degrees the surface is hydrophobic [26, 27, 28]. The contact angle of initial surface was 39.3 ± 0.9 degrees, whereas the one of the textured surface has increased to 42.8 ± 0.8 degrees. The silicon surface has been become less hydrophilic.

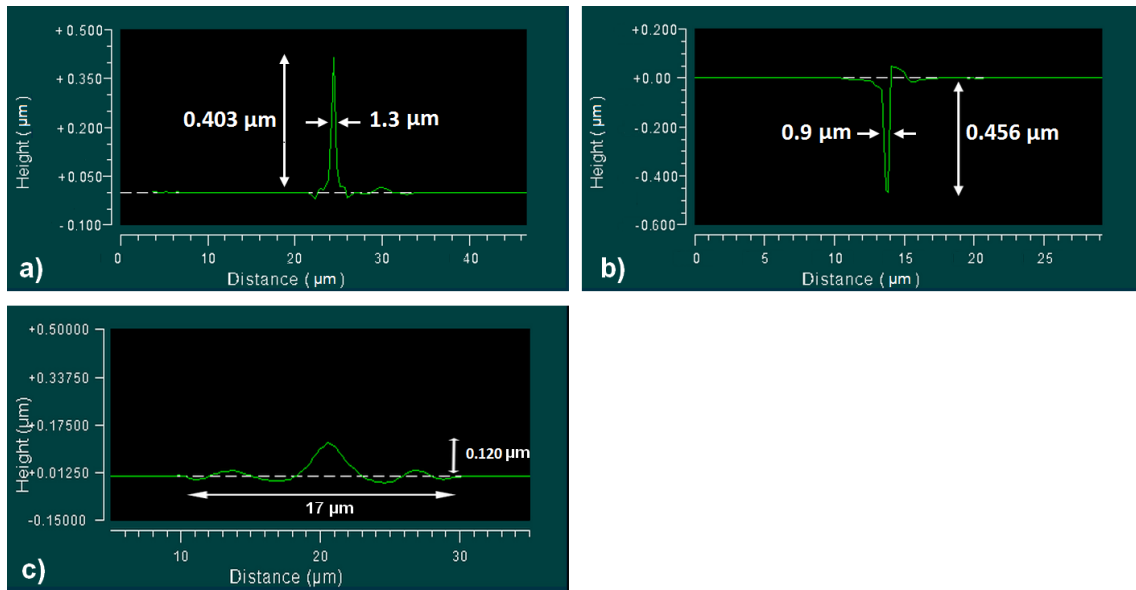


Figure 3: Examples of profiles on silicon with the Zygo microscope: a) a micro-peak; 35 pulses; pulse energy of $30 \mu\text{J}$; tip-sample distance of $100 \mu\text{m}$ — b) an ablation; 35 pulses; pulse energy of $36 \mu\text{J}$; tip-sample distance of $+100 \mu\text{m}$ — c) damage area without peak; pulse energy of $30 \mu\text{J}$; tip-sample distance of $110 \mu\text{m}$. Note that the unit lengths are not the same in the x and y axes.

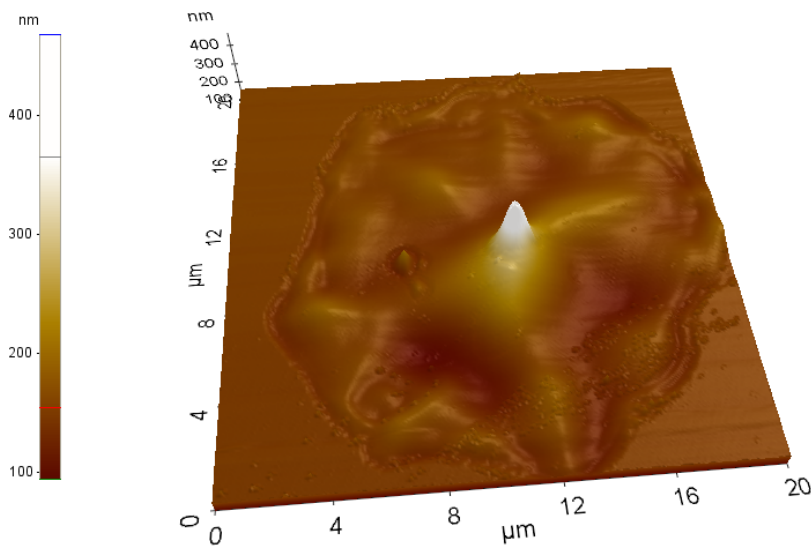


Figure 4: 3D view with the AFM. Example of a micro-peaks on silicon. Height of $335 \pm 2 \text{ nm}$, width $1.330 \pm 0.040 \mu\text{m}$, apex radius of $14 \pm 2 \text{ nm}$ — 35 pulses — pulse energy of $30 \mu\text{J}$.

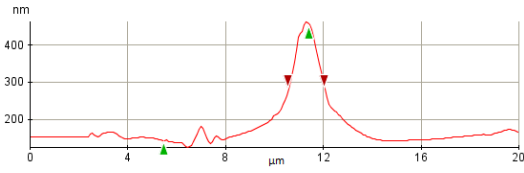


Figure 5: Example of a micro-peak profile on silicon with the AFM. Height of 335 ± 2 nm, width of 1.330 ± 0.040 μm , apex radius of 14 ± 2 nm; 35 pulses; pulse energy of 30 μJ .

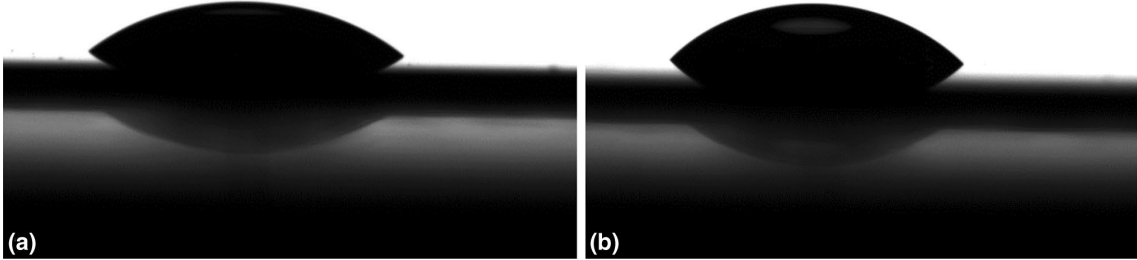


Figure 6: A drop of water ($\simeq 10$ μL) on: a) a non-textured silicon wafer; contact angle of 39.3 ± 0.9 degrees – b) the silicon wafer with micro-peaks, contact angle of 42.8 ± 0.8 degrees.

4 Conclusion

Direct micro-spikes machining by photonic jet using nanosecond laser pulses have been observed. Repeatable micro-peaks have been fabricated by 35 pulses of 100 nanoseconds at 1064 nm with a photonic jet generated in the vicinity of an shaped optical fiber tip. They are obtained on silicon with 30 μJ per pulses slightly under the ablation threshold (36 μJ). An hypothesis is that micro-peaks are formed due to hydrodynamic flow of molten material governed by surface-tension forces. This will be investigated. The potential of these micro-peaks for reducing the hydrophilicity of silicon has been illustrated.

Acknowledgment The authors are grateful to Camille Hairaye (ICube Laboratory, France) for her technical assistance in the use of the characterization system of wettability.

References

- [1] A. Abdurrochman, S. Lecler, F. Mermet, B. Y. Tumbelaka, B. Serio, and J. Fontaine, “Photonic jet breakthrough for direct laser microetching using nanosecond near-infrared laser,” *Appl. Opt.*, vol. 53, pp. 7202–7207, Nov 2014.
- [2] H.-J. Münzer, M. Mosbacher, M. Bertsch, J. Zimmermann, P. Leiderer, and J. Boneberg, “Local field enhancement effects for nanostructuring of surfaces,” *Journal of Microscopy*, vol. 202, no. 1, pp. 129–135, 2001.
- [3] W. Wu, A. Katsnelson, O. G. Memis, and H. Mohseni, “A deep sub-wavelength process for the formation of highly uniform arrays of nanoholes and nanopillars,” *Nanotechnology*, vol. 18, no. 48, p. 485302, 2007.

- [4] W. Guo, Z. B. Wang, L. Li, D. J. Whitehead, B. S. Luk'yanchuk, and Z. Liu, "Near-field laser parallel nanofabrication of arbitrary-shaped patterns," *Appl. Phys. Lett.*, vol. 90, p. 243101, June 2007.
- [5] D. Grojo, L. Charmasson, A. Pereira, M. Sentis, and P. Delaporte, "Monitoring Photonic Nanojets from Microsphere Arrays by Femtosecond Laser Ablation of Thin Films," *Journal of Nanoscience and Nanotechnology*, vol. 11, pp. 9129–9135, Oct. 2011.
- [6] E. Mcleod and C. B. Arnold, "Subwavelength direct-write nanopatterning using optically trapped microspheres," *Nature Nanotechnology*, vol. 3, pp. 413–417, July 2008.
- [7] J. Zelgowski, A. Abdurrochman, F. Mermet, P. Pfeiffer, J. Fontaine, and S. Lecler, "Photonic jet subwavelength etching using a shaped optical fiber tip," *Opt. Lett.*, vol. 41, pp. 2073–2076, May 2016.
- [8] R. Pierron, S. Lecler, J. Zelgowski, P. Pfeiffer, F. Mermet, and J. Fontaine, "Etching of semiconductors and metals by the photonic jet with shaped optical fiber tips," *Applied Surface Science*, vol. 418, Part B, pp. 452 – 455, 2017.
- [9] R. Pierron, J. Zelgowski, P. Pfeiffer, J. Fontaine, and S. Lecler, "Photonic jet: key role of injection for etchings with a shaped optical fiber tip," *Optics Letters*, vol. 42, no. 14, 2017.
- [10] Z. Chen, A. Taflove, and V. Backman, "Photonic nanojet enhancement of backscattering of light by nanoparticles: a potential novel visible-light ultramicroscopy technique," *Opt. Express*, vol. 12, pp. 1214–1220, Apr 2004.
- [11] S. Lecler, Y. Takakura, and P. Meyrueis, "Properties of a three-dimensional photonic jet," *Opt. Lett.*, vol. 30, pp. 2641–2643, Oct 2005.
- [12] A. V. Itagi and W. A. Challener, "Optics of photonic nanojets," *J. Opt. Soc. Am. A*, vol. 22, pp. 2847–2858, Dec 2005.
- [13] X. Li, Z. Chen, A. Taflove, and V. Backman, "Optical analysis of nanoparticles via enhanced backscattering facilitated by 3-d photonic nanojets," *Opt. Express*, vol. 13, pp. 526–533, Jan 2005.
- [14] A. Heifetz, S.-C. Kong, A. V. Sahakian, A. Taflove, and V. Backman, "Photonic Nanojets," *Journal of Computational and Theoretical Nanoscience*, vol. 6, pp. 1979–1992, Sept. 2009.
- [15] T.-H. Her, R. J. Finlay, C. Wu, S. Deliwala, and E. Mazur, "Microstructuring of silicon with femtosecond laser pulses," *Applied Physics Letters*, vol. 73, pp. 1673–1675, Sept. 1998.
- [16] D. S. Ivanov, B. Rethfeld, G. M. O'Connor, T. J. Glynn, A. N. Volkov, and L. V. Zhigilei, "The mechanism of nanobump formation in femtosecond pulse laser nanostructuring of thin metal films," *Applied Physics A*, vol. 92, no. 4, pp. 791–796, 2008.
- [17] A. I. Kuznetsov, J. Koch, and B. N. Chichkov, "Nanostructuring of thin gold films by femtosecond lasers," *Applied Physics A*, vol. 94, no. 2, pp. 221–230, 2009.
- [18] C. Unger, J. Koch, L. Overmeyer, and B. N. Chichkov, "Time-resolved studies of femtosecond-laser induced melt dynamics," *Opt. Express*, vol. 20, pp. 24864–24872, Oct 2012.

- [19] J. Zhu, W. Li, M. Zhao, G. Yin, X. Chen, D. Chen, and L. Zhao, "Silicon microstructuring using ultrashort laser pulses," in *Proceedings of SPIE*, 2005.
- [20] A. I. Kuznetsov, C. Unger, J. Koch, and B. N. Chichkov, "Laser-induced jet formation and droplet ejection from thin metal films," *Applied Physics A*, vol. 106, no. 3, pp. 479–487, 2012.
- [21] J. P. Moening, S. S. Thanawala, and D. G. Georgiev, "Formation of high-aspect-ratio protrusions on gold films by localized pulsed laser irradiation," *Applied Physics A*, vol. 95, no. 3, pp. 635–638, 2009.
- [22] J. P. Moening, D. G. Georgiev, and J. G. Lawrence, "Focused ion beam and electron microscopy characterization of nanosharp tips and microbumps on silicon and metal thin films formed via localized single-pulse laser irradiation," *Journal of Applied Physics*, vol. 109, p. 014304, Jan. 2011.
- [23] L. M. Borsuk, "Alternating current arc for lensing system and method of using same," May 1988.
- [24] B. K. Nayak, P. O. Caffrey, C. R. Speck, and M. C. Gupta, "Superhydrophobic surfaces by replication of micro/nano-structures fabricated by ultrafast-laser-microtexturing," *Applied Surface Science*, vol. 266, pp. 27 – 32, 2013.
- [25] C. Hairaye, F. Mermet, T. Engel, P. C. Montgomery, and J. Fontaine, "Functionalization of surfaces by ultrafast laser micro/nano structuring," *Journal of Physics: Conference Series*, vol. 558, no. 1, p. 012063, 2014.
- [26] T. Young, "An Essay on the Cohesion of Fluids," *Philosophical Transactions of the Royal Society of London*, vol. 95, pp. 65–87, Jan. 1805.
- [27] R. N. Wenzel, "Resistance of solid surfaces to wetting by water," *Industrial & Engineering Chemistry*, vol. 28, pp. 988–994, Aug. 1936.
- [28] A. B. D. Cassie and S. Baxter, "Wettability of porous surfaces," *Trans. Faraday Soc.*, vol. 40, pp. 546–551, 1944.